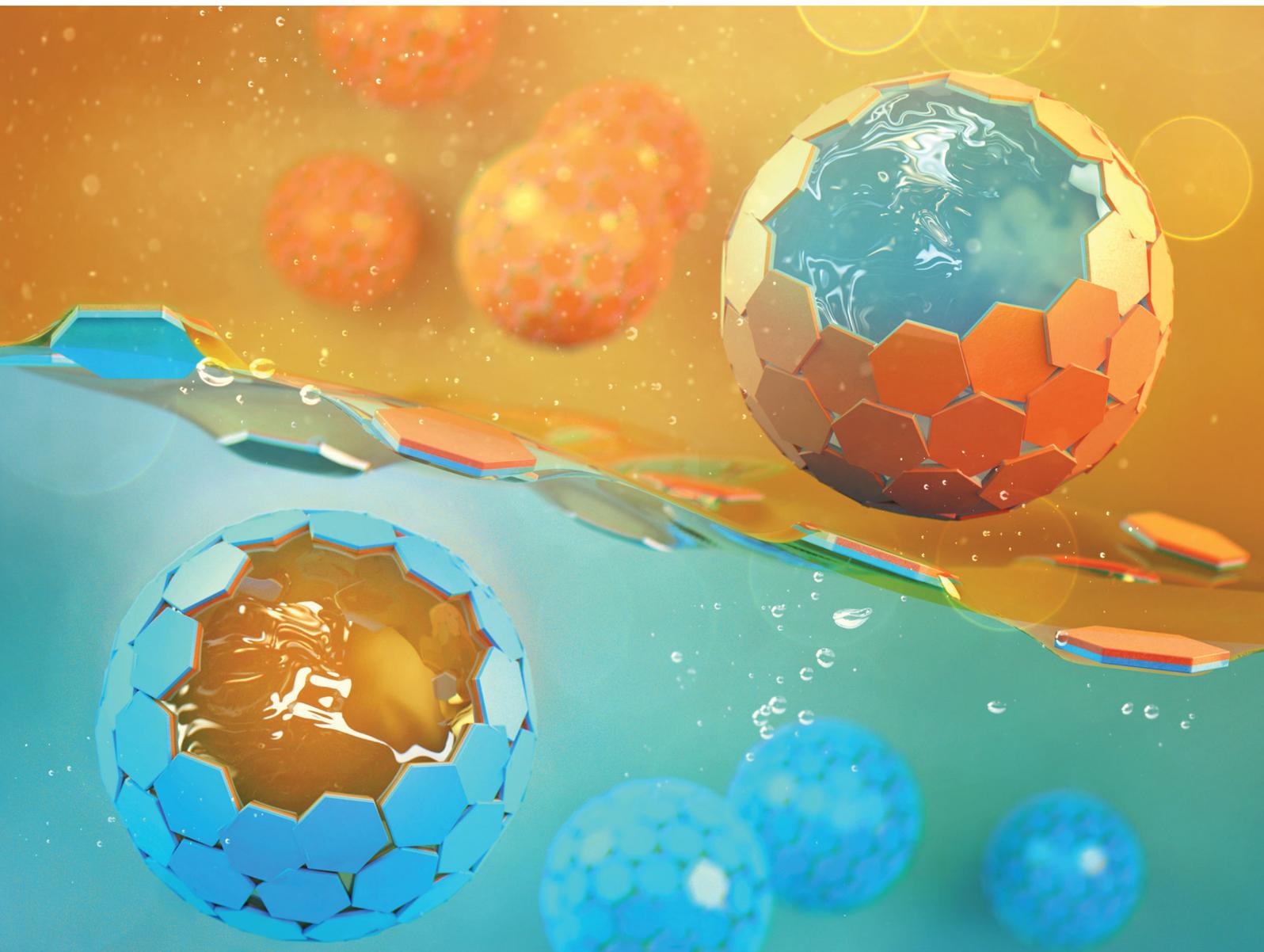# ChemComm

Chemical Communications

ROYAL SOCIETY
OF CHEMISTRY

COMMUNICATION
Bum Jun Park, Jin Woong Kim *et al.*
Janus amphiphilic nanoplatelets as smart colloid surfactants
with complementary face-to-face interactions

Check for updates

Janus amphiphilic nanoplatelets as smart colloid surfactants with complementary face-to-face interactions†

Jin Yong Lee,‡[a] Kyu Hwan Choi,‡[b] Jaemin Hwang,[c] Minchul Sung,[c] Ji Eun Kim,[a] Bum Jun Park [ID] *[b] and Jin Woong Kim [ID] *[c]

We introduce amphiphilic nanoplatelets (ANPLs) that not only have a nanoscale Janus platelet geometry, but can also induce complementary face-to-face interactions among Pickering emulsion droplets. We showed that the ANPLs with such high surface activity can be a promising colloid surfactant enabling smart rheology modification of complex emulsion fluids.

Emulsion systems in which deformable drops are dispersed in a liquid continuous phase can exhibit a solid-like rheological behaviour analogous to that of a suspension of hard spheres, although this critically depends on the volume fraction of the dispersed drops (ϕ_d). If the dispersed liquid drops are clustered and successfully form a three-dimensional network, a solid-like emulsion gel phase is generated even at low ϕ_d.[1–3] Such a network made up of drop clusters is typically obtained by inducing the dipole–dipole attraction between drops or by incorporating polymer depletants.[4–12] In terms of tightly controlling the phase characteristics of emulsions by introducing designated interaction sites on the droplet surface, the use of Pickering emulsions is very attractive.[13,14] Depending on the size, shape, wettability, and Janusity of solid particles assembled at the oil–water interface, the association between drops is readily manipulated in a controlled manner.[15–25] From a rheological point of view, the fluidity of Pickering emulsions is also affected by ϕ_d. Once the solid particles strongly adsorb at the interface, a Pickering emulsion having a high internal phase with $\phi_d > 0.7$ can be obtained, while displaying superior gelation in spite of quite low concentrations of particles.[26–30] In this case, to develop a structurally stable solid-like Pickering emulsion at low ϕ_d, the solid particles must have a strong

adsorption capacity at the interface and at the same time induce weak but effective attraction between the particles – called armoured droplets.[31–33] To meet these requirements, it is crucial to develop a new type of Pickering emulsion system in which solid particles not only adsorb at the interface with perfect wetting, but also have the ability to effectively trigger mutual attraction between droplets.

Herein, we propose a nanoplatelet surfactant-armoured emulsion Pickering gel system, in which amphiphilic nanoplatelets (ANPLs) are employed as an attractive particulate surfactant. The uniqueness and novelty of the ANPLs are that they have a Janus nanoplatelet geometry as well as an amphiphilic Janus structure, thus they behave like a surfactant with very high adhesion energy at the oil–water interface.[34] Once an extremely stable ANPL-armoured Pickering emulsion system is established, its phase properties are tuneable regardless of the oil-in-water (O/W) or water-in-oil (W/O) emulsion type. Any emulsion type can be manipulated by solely taking advantage of the face-to-face interactions between ANPLs attached to different droplets, as illustrated in Fig. 1. Finally, we attempt to demonstrate that the interactions between ANPLs played a key role in modifying the suspension rheology of attractive Pickering emulsion gels.

In our typical synthesis of the ANPLs (see the ESI†), we first incorporated surface initiation sites on bare zirconium hydrogen phosphate (ZrHP) nanoplatelets (NPLs) and then used surface-induced activators regenerated by electron transfer atom transfer radical polymerization (SI-ARGET ATRP) at the O/W interface stabilized with ZrHP NPLs (Fig. S1, ESI†).[35,36] Incorporation of initiation sites was confirmed by observing N from the ZrHP NPLs in the X-ray photoelectron spectroscopy spectra (Fig. S2a, ESI†). After SI-ARGET ATRP, grafting of poly(poly(ethylene glycol)methacrylate) (pPEGMA, nonionic type) or poly(PEGMA-*co*-2-aminoethyl methacrylate) (p(PEGMA-*co*-AMA), ionic type) hydrophilic brushes on one surface plane of the ZrHP NPLs and poly(butyl methacrylate) (pBMA) hydrophobic brushes on the other plane was characterized by zeta potential (Fig. S2b, ESI†) and thermogravimetric analyses (Fig. S3, ESI†).

[a] *Department of Bionano Technology, Hanyang University, Ansan, 15588, Republic of Korea*

[b] *Department of Chemical Engineering, Kyung Hee University, Yongin, 17104, Republic of Korea. E-mail: bjpark@khu.ac.kr*

[c] *School of Chemical Engineering, Sungkyunkwan University, Suwon, 16419, Republic of Korea. E-mail: jinwoongkim@skku.edu*

† Electronic supplementary information (ESI) available. See DOI: 10.1039/d0cc02231d

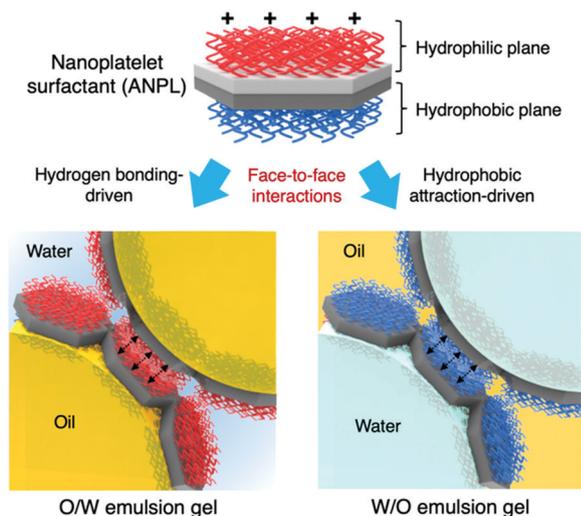‡ These authors equally contributed to this work.

Fig. 1 Schematic illustration for the formation of Pickering emulsion gels depending on the selective attraction between ANPL planes.

Even after ARGET ATRP, the ANPLs retained their original platelet morphology with a diameter of ~300 nm (Fig. 2a and b). The height changes before and after the selective incorporation of hydrophilic and hydrophobic polymer brushes were also measured by AFM observation (Fig. 2c–f). The thickness of the bare ZrHP NPLs and ANPLs was measured to be ~20 and ~39 nm, respectively, indicating that the polymer brush layers were generated with a thickness of ~9.5 nm. Furthermore, one hydrophilic plane of the ANPLs was selectively labelled with a fluorescent dye to conduct CLSM observation of the electrostatic interaction
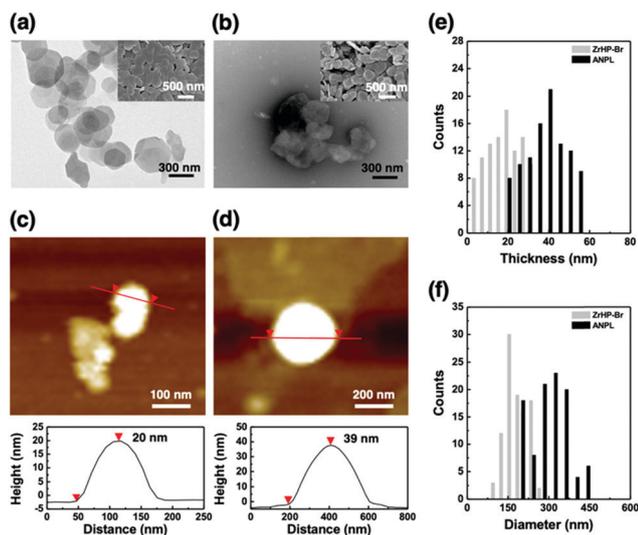
between fluorescein sodium salt and cationic moieties of p(PEGMA-co-AMA). This revealed that the ANPLs had amphiphilic Janus platelet morphology with potential to selectively decorate one of the platelet surfaces with functional moieties (Fig. S4, ESI†).

In general, the stability of Pickering emulsions is determined by the attachment energy of particles at the liquid–liquid interface. Platelet-shaped particles are expected to lie flat at the interface due to their preferred orientation, which is quite comparable to spherical particles.[30] To quantitatively understand the configuration behaviours of ANPLs at the oil–water interface, their attachment energy was numerically calculated as a function of the orientation angle (φ) and the vertical displacement (d_{I}) using the Hit-and-Miss Monte Carlo method (see the ESI†).[37] As shown in Fig. 3a, the global energy minimum was found in the upright configuration at $\varphi = 0°$, in which the ANPL's hydrophilic plane contacts with the interface and all other parts are wetted by the oil phase. The magnitude of the energy minimum was obtained as ~$-10^6 \, k_{\mathrm{B}}T$ that is energetically strong enough for the ANPL to irreversibly adhere to the interface. The secondary energy minimum was observed for the inverted configuration at $\varphi = 180°$. In this case, the hydrophobic plane is in contact with the interface, and the other surfaces are exposed to the oil phase. The tendency of the ANPL to prefer the oil phase the equilibrium condition is due to the fact that the side region of the ANPL is in a close to neutral
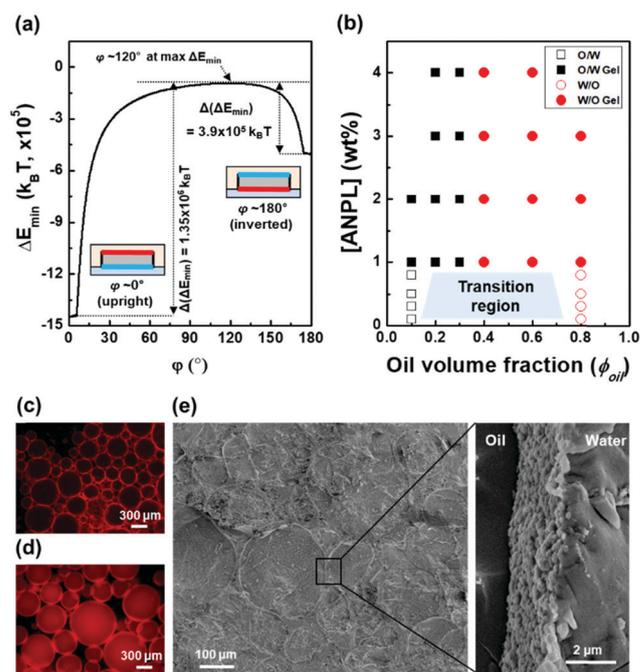

Fig. 2 Morphological observation of bare ZrHP−Br NPLs and ANPLs with hydrophilic p(PEGMA-co-AMA) brushes and hydrophobic pBMA brushes. TEM images of (a) bare ZrHP−Br NPLs and (b) ANPLs. The insets show SEM images of the corresponding TEM images. AFM images of (c) ZrHP−Br NPLs and (d) ANPLs. The line analysis of the height profiles of ZrHP−Br NPLs and ANPLs. Statistics of (e) platelet thickness and (f) diameter of ZrHP−Br NPLs and ANPLs measured via AFM. In this study, ANPLs with p(PEGMA-co-AMA) and pBMA brushes were used.

Fig. 3 (a) Determination of energetically favourable configurations of ANPLs at the oil–water interface. (b) Apparent phase diagram of ANPL-armoured Pickering emulsions. Fluorescence microscopy images of ANPL-armoured Pickering emulsions: (c) O/W emulsion drops with Nile red in n-decane dispersed phase and (d) W/O emulsion with dextran tetramethylrhodamine in water dispersed phase. (e) Cryo-SEM images of an ANPL-armoured O/W emulsion. $\phi_{\mathrm{oil}} = 0.2$. [ANPL] = 4 wt%. ANPLs with p(PEGMA-co-AMA) and pBMA brushes were used for these observations.

wetting state but is slightly hydrophobic (*i.e.*, $\theta_S = 93.5°$ in Fig. S5, ESI†). The presence of the two energy minima indicates that the probability of the two configurations would be stochastically determined. This implies that when the ANPL falls into the secondary energy minimum adopting the inverted configuration, it cannot spontaneously flip over to take the upright configuration due to the presence of a high-energy barrier of $\Delta(\Delta E_{min}) = 3.9 \times 10^5 \, k_B T$ between the two configurations. In other words, once the ANPL is adsorbed at the oil–water interface, it can enhance the structural stability of the emulsion without any desorption. Note that if the wettability of the ANPL side is near-neutral but slightly hydrophilic (*e.g.*, $\theta_S = 86.5°$), the ANPL prefers to be in the aqueous phase rather than the oil phase, and the primary and secondary energy minima are identically found in the upright and inverted configurations, respectively (Fig. S5 and S6, ESI†). The near-neutral wettability of the side region suggests that the position of the ANPL relative to the interface can be sensitively affected by external disturbance. For example, the emulsion types of O/W *versus* W/O likely depend on the relative amounts of water and oil in the emulsion preparation.

Based on this theoretical understanding of ANPL interfacial adsorption, we then observed the actual Pickering emulsion formation behaviours with varying ANPL concentration and ϕ_{oil} (Fig. 3b and Fig. S7, S8, ESI†). Through apparent observation, when the ANPL concentration was less than 1 wt%, we confirmed the transition region in the range of $\phi_{oil} = 0.1$–0.8, where the emulsion type could be either O/W or W/O. Strikingly, when the ANPL concentration was over 1 wt%, the gelation of emulsion drops occurred in the range of $\phi_{oil} = 0.2$–0.3. The typical transition of emulsion types was observed at $\phi_{oil} = 0.3$–0.4 (Fig. 3c, d and Fig. S8, ESI†). From cryo-SEM observation, we could directly confirm that the ANPLs were oriented along the interface to form a buckled layer (Fig. 3e). Thanks to this tight interfacial orientation, the ANPL-armoured Pickering emulsions exhibited improved emulsion stability (Fig. S9, ESI†).

The ANPL-armoured Pickering emulsions prepared in this study showed the formation of droplet clusters followed by creaming for O/W emulsions or sedimentation for W/O emulsions (Fig. 4a and Fig. S7, ESI†). For example, in the case of the O/W Pickering emulsions prepared using 0.1–0.5 wt% ANPLs, the oil drops directly associated with each other to form a macroscopic cluster without coalescence or break-up. This huge emulsion cluster was able to recover to its original emulsion state upon gentle shaking. When using more than 2 wt% ANPLs, a typical solid-like emulsion gel phase was generated. To characterize this unprecedented gelation of ANPL-armoured Pickering emulsions more clearly, we carried out rheological measurements. It was surprising to notice that although there was a difference in the gel strength depending on ϕ_{oil} and ANPL concentration, all the Pickering emulsions showed $G' > G''$. This occurred regardless of the emulsion type in the wide range of $\phi_{oil} = 0.1$–0.8 and from very diluted ANPL concentrations, which indicates that a solid-like emulsion gel phase was generated (Fig. 4b and c). Presumably, this unique gelation behaviour was driven by the ANPLs covering the drops. For the ANPL-armoured O/W emulsion
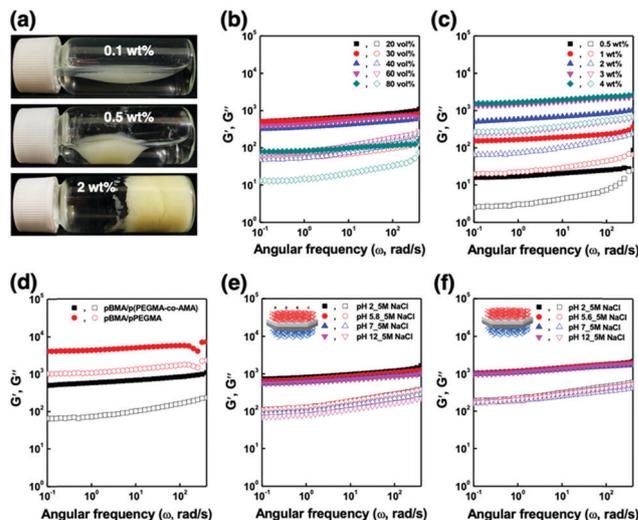

Fig. 4 (a) Formation of a macroscopic cluster and emulsion of ANPL-armoured Pickering emulsion drops prepared with changing ANPL concentration. Storage modulus, G' (closed symbols), and loss modulus, G'' (open symbols), of ANPL-armoured Pickering emulsions with varying oscillation frequency: effects of (b) ϕ_{oil} at fixed [ANPL] = 2 wt% and (c) [ANPL] at fixed $\phi_{oil} = 0.2$ and (d) comparison of the relative degree of attraction between hydrophilic polymer brushes on the ANPLs. Tolerance to pH and salinity changes at fixed [ANPL] = 2 wt% and $\phi_{oil} = 0.2$: (e) ANPLs with p(PEGMA-*co*-AMA) and pBMA brushes and (f) ANPLs with p(PEGMA) and pBMA brushes.

system, we assume that the p(PEGMA-*co*-AMA) brush-grafted hydrophilic plane of the ANPLs has many hydrogen bonding sites. Therefore, the ANPLs can possibly induce an oil drop-to-oil drop attraction across the continuous phase. To experimentally support this assumption, we prepared Pickering emulsions stabilized with pPEGMA brush-grafted ANPLs, which had more hydrogen bonding sites than the p(PEGMA-*co*-AMA) brush-grafted ones. We could observe from the rheological studies that the pPEGMA brush-grafted ANPL-armoured Pickering emulsions showed a further increase in moduli of about one order of magnitude compared with the p(PEGMA-*co*-AMA) brush-grafted ANPL-armoured emulsions (Fig. 4d and Fig. S10, ESI†), confirming again that hydrogen bonding-driven face-to-face attraction between ANPLs surrounding the droplets led to the generation of the Pickering emulsion gels. In the case of the ANPL-armoured W/O emulsion system, following a similar interaction mechanism, hydrophobic attraction would occur favourably between the pBMA brushes on the hydrophobic plane of the ANPLs on the water drops through the *n*-decane oil continuous phase. Thus, this should produce relatively weak W/O emulsion gels, compared with O/W emulsion gels with the same composition. Consequently, it is natural that our ANPL-armoured Pickering emulsions possessing these structural and phasic features would have excellent tolerance to changes in medium pH and salinity (Fig. 4e and f).

In summary, we have reported new platelet surfactants, ANPLs. We showed that the platelet particles strongly and irreversibly attached to the oil–water interface and their morphology with amphiphilicity greatly enhanced the structural stability of the

Pickering emulsions. We also found that the ANPL-armoured Pickering emulsions could be gelled by taking advantage of either hydrogen bonding-driven attraction or hydrophobic attraction between ANPLs surrounding the droplets. These results highlight that our nanoplatelet surfactant system would find great applicability in the fields of personal care formulations as well as interfacial catalytic activity-based microreactions.

Conflicts of interest

There are no conflicts to declare.

Notes and references

1 T. G. Mason, J. Bibette and D. A. Weitz, *Phys. Rev. Lett.*, 1995, **75**, 2051–2054.
2 T. G. Mason, J. N. Wilking, K. Meleson, C. B. Chang and S. M. Graves, *J. Phys.: Condens. Matter*, 2006, **18**, R635–R666.
3 R. Foudazi, S. Qavi, I. Masalova and A. Y. Malkin, *Adv. Colloid Interface Sci.*, 2015, **220**, 78–91.
4 M. J. Solomon and P. T. Spicer, *Soft Matter*, 2010, **6**, 1391–1400.
5 S. Minami, T. Watanabe, D. Suzuki and K. Urayama, *Soft Matter*, 2018, **14**, 1596–1607.
6 T. Yan, K. Schröter, F. Herbst, W. H. Binder and T. Thurn-Albrecht, *Macromolecules*, 2014, **47**, 2122–2130.
7 N. M. James, E. Han, R. A. L. de la Cruz, J. Jureller and H. M. Jaeger, *Nat. Mater.*, 2018, **17**, 965–970.
8 R. Mezzenga, P. Schurtenberger, A. Burbidge and M. Michel, *Nat. Mater.*, 2005, **4**, 729–740.
9 Y. Qin, R. Chang, S. Ge, L. Xiong and Q. Sun, *Int. J. Biol. Macromol.*, 2017, **102**, 1073–1082.
10 Y. R. Lee, D. Park, S. K. Choi, M. Kim, H. S. Baek, J. Nam, C. B. Chung, C. O. Osuji and J. W. Kim, *ACS Appl. Mater. Interfaces*, 2017, **9**, 31095–31101.
11 F. Oliveira, S. R. Monteiro, A. Barros-Timmons and J. A. Lopes-da-Silva, *Carbohydr. Polym.*, 2010, **82**, 1219–1227.
12 J. Y. Lee, M. Sung, H. Seo, Y. J. Park, J. B. Lee, S. S. Shin, Y. Lee, K. Shin and J. W. Kim, *J. Ind. Eng. Chem.*, 2020, **86**, 158–166.
13 S. U. Pickering, *J. Chem. Soc., Trans.*, 1907, **91**, 2001–2021.
14 B. P. Binks, *Curr. Opin. Colloid Interface Sci.*, 2002, **7**, 21–41.
15 J. W. Kim, J. Cho, J. Cho, B. J. Park, Y. J. Kim, K. H. Choi and J. W. Kim, *Angew. Chem., Int. Ed.*, 2016, **55**, 4509–4513.
16 J. W. Kim, R. J. Larsen and D. A. Weitz, *J. Am. Chem. Soc.*, 2006, **128**, 14374–14377.
17 J. W. Kim, D. Lee, H. C. Shum and D. Weitz, *Adv. Mater.*, 2008, **20**, 3239–3243.
18 A. Walther and A. H. Muller, *Chem. Rev.*, 2013, **113**, 5194–5261.
19 S. Jiang, Q. Chen, M. Tripathy, E. Luijten, K. S. Schweizer and S. Granick, *Adv. Mater.*, 2010, **22**, 1060–1071.
20 K. H. Roh, D. C. Martin and J. Lahann, *Nat. Mater.*, 2005, **4**, 759–763.
21 J. Hu, S. Zhou, Y. Sun, X. Fang and L. Wu, *Chem. Soc. Rev.*, 2012, **41**, 4356–4378.
22 Z. Nie, W. Li, M. Seo, S. Xu and E. Kumacheva, *J. Am. Chem. Soc.*, 2006, **128**, 9408–9412.
23 F. Wurm and A. F. Kilbinger, *Angew. Chem., Int. Ed.*, 2009, **48**, 8412–8421.
24 A. H. Groschel, A. Walther, T. I. Lobling, J. Schmelz, A. Hanisch, H. Schmalz and A. H. Muller, *J. Am. Chem. Soc.*, 2012, **134**, 13850–13860.
25 A. Walther, K. Matussek and A. H. Muller, *ACS Nano*, 2008, **2**, 1167–1178.
26 P. J. Colver and S. A. Bon, *Chem. Mater.*, 2007, **19**, 1537–1539.
27 E. Perrin, H. Bizot, B. Cathala and I. Capron, *Biomacromolecules*, 2014, **15**, 3766–3771.
28 B. Jiao, A. Shi, Q. Wang and B. P. Binks, *Angew. Chem., Int. Ed.*, 2018, **57**, 9274–9278.
29 D. Cai, J. H. Thijssen and P. S. Clegg, *ACS Appl. Mater. Interfaces*, 2014, **6**, 9214–9219.
30 J. Lee and J. Y. Chang, *Chem. Eng. J.*, 2020, **381**, 122767.
31 K. Kim, S. Kim, J. Ryu, J. Jeon, S. G. Jang, H. Kim, D. G. Gweon, W. B. Im, Y. Han, H. Kim and S. Q. Choi, *Nat. Commun.*, 2017, **8**, 14305.
32 F. Liu, J. Zheng, C.-H. Huang, C.-H. Tang and S.-Y. Ou, *Food Hydrocolloids*, 2018, **82**, 96–105.
33 M. A. Creighton, Y. Ohata, J. Miyawaki, A. Bose and R. H. Hurt, *Langmuir*, 2014, **30**, 3687–3696.
34 F. Liang, K. Shen, X. Qu, C. Zhang, Q. Wang, J. Li, J. Liu and Z. Yang, *Angew. Chem., Int. Ed.*, 2011, **50**, 2379–2382.
35 B. Liu, W. Wei, X. Qu and Z. Yang, *Angew. Chem., Int. Ed.*, 2008, **47**, 3973–3975.
36 X. N. Huang, F. Z. Zhou, T. Yang, S. W. Yin, C. H. Tang and X. Q. Yang, *Food Hydrocolloids*, 2019, **93**, 34–45.
37 B. J. Park and D. Lee, *ACS Nano*, 2012, **6**, 782–790.